Single-crystalline $B_{12}As_2$ on *m*-plane $(1\bar{1}00)$ 15*R*-SiC

Hui Chen,[1,a)] Guan Wang,[1] Michael Dudley,[1] Zhou Xu,[2] J. H. Edgar,[2] Tim Batten,[3] Martin Kuball,[3] Lihua Zhang,[4] and Yimei Zhu[4]
[1]*Department of Materials Science and Engineering, Stony Brook University, Stony Brook, New York 11794, USA*
[2]*Department of Chemical Engineering, Kansas State University, Manhattan, Kansas 66506, USA*
[3]*H.H. Wills Physics Laboratory, University of Bristol, Bristol BS8 1TL, United Kingdom*
[4]*Center for Functional Materials, Brookhaven National Laboratory, Upton, New York 11973, USA*

(Received 10 May 2008; accepted 24 May 2008; published online 13 June 2008)

Single crystal, heteroepitaxial growth of icosahedral $B_{12}As_2$ (IBA, a boride semiconductor) on *m*-plane 15*R*-SiC is demonstrated. Previous studies of IBA on other substrates, i.e., (111)Si and (0001)6*H*-SiC, produced polycrystalline and twinned epilayers. In contrast, single-crystalline and untwinned IBA was achieved on *m*-plane 15*R*-SiC. Synchrotron white beam x-ray topography, Raman spectroscopy, and high resolution transmission electron microscopy confirm the high quality of the films. High quality growth is shown to be mediated by ordered nucleation of IBA on (474) substrate facets. This work demonstrates that *m*-plane 15*R*-SiC is a good substrate choice to grow high-quality untwinned IBA epilayers for future device applications. © *2008 American Institute of Physics*. [DOI: 10.1063/1.2945635]

Icosahedral boron arsenide $B_{12}As_2$ (IBA) is a wide band gap semiconductor (3.47 eV) with the extraordinary ability to "self-heal" radiation damage. This makes it an attractive choice for devices exposed to radiation which can severely degrade the electrical properties of conventional semiconductors, causing devices to cease functioning. Among the particularly intriguing possible applications for IBA are beta cells, devices capable of producing electrical energy by coupling a radioactive beta emitter to a semiconductor junction, another space electronics.[1–8] IBA is based on 12-boron-atom icosahedra, which reside at the corners of an α-rhombohedral unit cell, and two-atom As–As chains lying along the rhombohedral [111] axis.[1,5] In the absence of native substrates, IBA has been heteroepitaxially grown on substrates with compatible structural parameters. To date, this has been attempted on substrates with higher symmetry than IBA such as Si and 6*H*-SiC.[5,7–11] Unfortunately, growth of a lower symmetry epilayer on a higher symmetry substrate often produces structural variants, a phenomenon known as degenerate epitaxy.[12,13] These variants are expected to have a detrimental effect on device performance, and have severely hindered progress of this material to date.[5] An enumeration of these variants can be obtained by analysis of the two-dimensional (2D) point groups of the substrate surface and the epilayer surface.[13] For the case of IBA grown on Si with (100), (110), and (111) orientation and (0001) 6*H*-SiC, rotational and translational variants are both predicted and observed.[5,10,11] Use of offcut substrates potentially enables manipulation of the relative populations of the multiple variants, however, studies on offcut (0001) 6*H*-SiC substrates have so far been largely unsuccessful.[7,9] The effect of degenerate epitaxy, however, can also be used to advantage by choosing substrates for which no variants are predicted. Single terrace, *m*-plane 15*R*-SiC fulfils this requirement for IBA. In this letter, we report that IBA grown on *m*-plane 15*R*-SiC is free from structural variants and is of high single crystalline quality, offering a potential for future device applications.

IBA was deposited using chemical vapor deposition onto *m*-plane 15*R*-SiC at 1200 °C and 500 Torr of reactor pressure for 1 h, using 1% B_2H_6 in H_2 and 2% AsH_3 in H_2 as sources. The epitaxial IBA film had a nominal thickness of 3 μm. As large scale 15*R*-SiC substrates are presently not readily available, a commercial *m*-plane 6*H*-SiC substrate was used, which contained 15*R*-SiC inclusions of about 300–500 μm in diameter. The film/substrate orientations were determined by synchrotron white beam x-ray topography (SWBXT). Raman spectroscopy analysis of the films using a Renishaw InVia micro-Raman system with 488 nm laser excitation provided information on the SiC polytype and the relative quality of the IBA. The interfaces between the IBA and the SiC were examined by high-resolution transmission electron microscopy (HRTEM) using a 300 keV JEOL 3000EX system at Brookhaven National Laboratory.

SWBXT Laue patterns recorded from an IBA film on *m*-plane 15*R*-SiC provided global determination that the film was single crystal of (353) orientation and twin free. This constitutes a significant improvement over films grown under identical conditions on *m*-plane 6*H*-SiC.[14] Raman spectra, as shown in Fig. 1, confirm this improvement with the Raman linewidth being narrower for the IBA film grown on 15*R*-SiC, and in particular, Raman intensity is significantly stronger, despite both films having similar thickness. This illustrates that phonon properties, and therefore, also more macroscopic properties of the film, are improved.

Excellent crystal quality was confirmed using HRTEM. A representative image in Fig. 2 shows an abrupt, clean interface and no twins, in contrast to results from *m*-plane 6*H*-SiC.[14] Structural correspondence was confirmed using multislice simulation[11] and the lattice orientation observed is consistent with (353) film orientation. A single *m*-plane terrace of the 15*R*-SiC substrate surface (shown in cross section in Fig. 3, lower black line) exhibits a 2D point group *m*, while that of the (353) IBA is also *m*, so that no structural variants are predicted in agreement with the observed ab-

a)Electronic mail: huichen@ic.sunysb.edu.

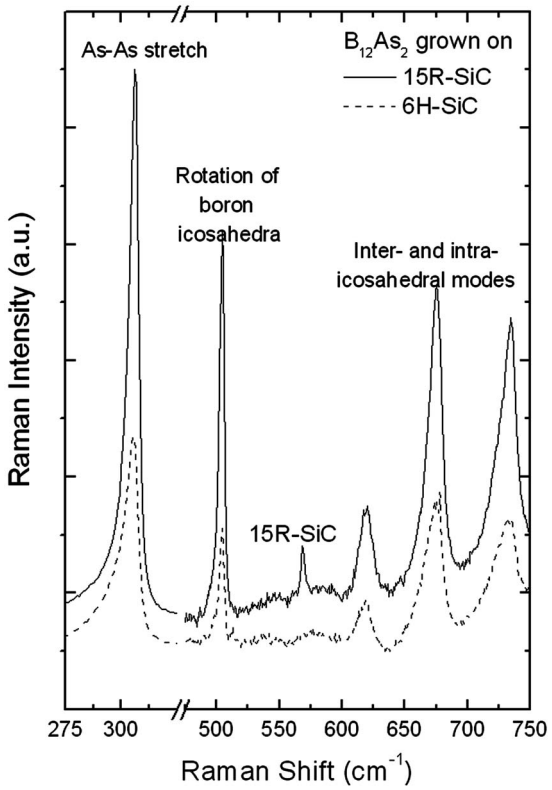

FIG. 1. Raman spectra recorded from IBA grown on *m*-plane 15*R*- and 6*H*-SiC. There are no 6*H*-SiC substrate modes in the spectral range shown, but one 15*R*-SiC mode.

sence of twins. However, the 15*R*-SiC substrate surface, hydrogen etched prior to growth, is expected to display a faceted structure featuring alternating close-packed (474) and (212) facets that are three and two bilayers wide, respectively, analogous to the behavior observed in *m*-plane 6*H*-SiC,[14,15] and why IBA growth is single-crystalline and untwinned therefore needs further explanation.

If the substrate surface was exclusively composed of (474) and (212) facets, the asymmetry in their widths would result in a ~3° offset from *m*-plane orientation (see Fig. 3, middle line). The periodic appearance of (11·8·11) facets would compensate for this asymmetry and produce an "on-axis" surface, as shown in Fig. 3 (upper line). This latter surface can be considered as quasivicinal with the (474) facets acting as terraces and the other facets as step risers. The stacking sequence below each (474) facet is identical such that the facets expose a series of equal thickness, lamellar nanodomains of 3C (cubic) structure leading to identical nucleation possibilities (see Fig. 3). This therefore breaks the symmetry of the *m*-plane surface, thus eliminating the associated advantage for IBA growth.

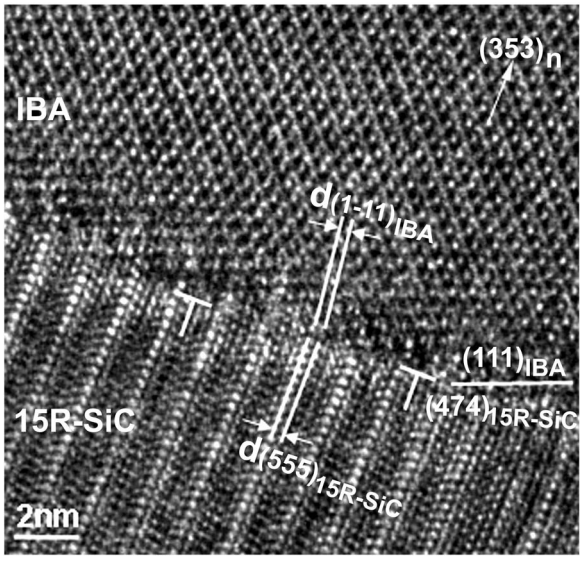

FIG. 2. HRTEM images recorded along the $[10\bar{1}]$ zone axis (parallel to $[11\bar{2}0]$ in the hexagonal system) showing a sharp IBA/15*R*-SiC interface and the (353) surface orientation of IBA. The symbol ⊥ marks the location of interfacial dislocations with extra half planes in the 15*R*-SiC substrate.

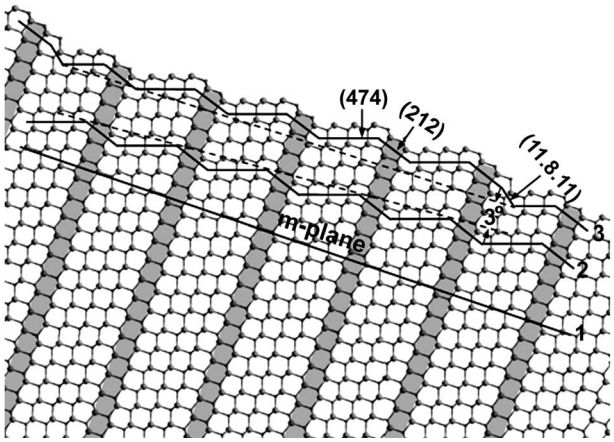

FIG. 3. Cross-sectional visualization along $[10\bar{1}]$ of the 15*R*-SiC structure. The uppermost black line indicates the on-axis, facet configuration comprising closed-packed (474) atomic terraces and coupled (212) and (11·8·11) step risers. The middle black line indicates the surface comprising only of (474) and (212) facets which result in a 3° misorientation from *m*-plane and the lower line indicates the *m*-plane itself (unfaceted). Note the lamellar nanodomains of 3*C*-SiC structure bounded by the (474) facets and the shaded domain boundaries parallel to the (111) plane [(0001) in hexagonal system].

In order to understand why the IBA adopts a highly crystalline, untwinned configuration on this substrate, it is instructive to consider the details of the substrate and IBA structures and, in particular, the dangling bond configurations exhibited at the interface. Straightforward consideration of lattice geometry reveals that if the IBA nucleates on either the broader $(474)_{15R\text{-}SiC}$ or the narrower $(212)_{15R\text{-}SiC}$ facets with the $(111)_{IBA}$ planes aligned to the facets, the film would adopt $(353)_{IBA}$ orientation in agreement with observations, although if nucleation occurs simultaneously on both types of facet, the film would be polycrystalline. However, the large dimension of the in-plane repeat unit of the $(111)_{IBA}$ (twice that of the close-packed SiC planes) requires that the facet width be large enough to accommodate nuclei of IBA which are at least two icosahedra wide [see Fig. 4(a)] so that preferential nucleation on the broader $(474)_{15R\text{-}SiC}$ facets is expected. Additional stabilization for nucleation on the $(474)_{15R\text{-}SiC}$ facets is provided by the fact that the IBA is able to simultaneously bond to the $(474)_{15R\text{-}SiC}$ terrace and the adjacent $(212)_{15R\text{-}SiC}$ step riser, as shown in Figs. 4(a) and 4(b). In contrast, such stabilization is absent for IBA nuclei in twinned orientation, thus, preventing nucleation of twins (see also Fig. 4). Therefore, the choice of $(353)_{IBA}$ orientation is dominated by the tendency to nucleate in $(111)_{IBA}$ orientation on close-packed substrate facets of sufficient breadth.

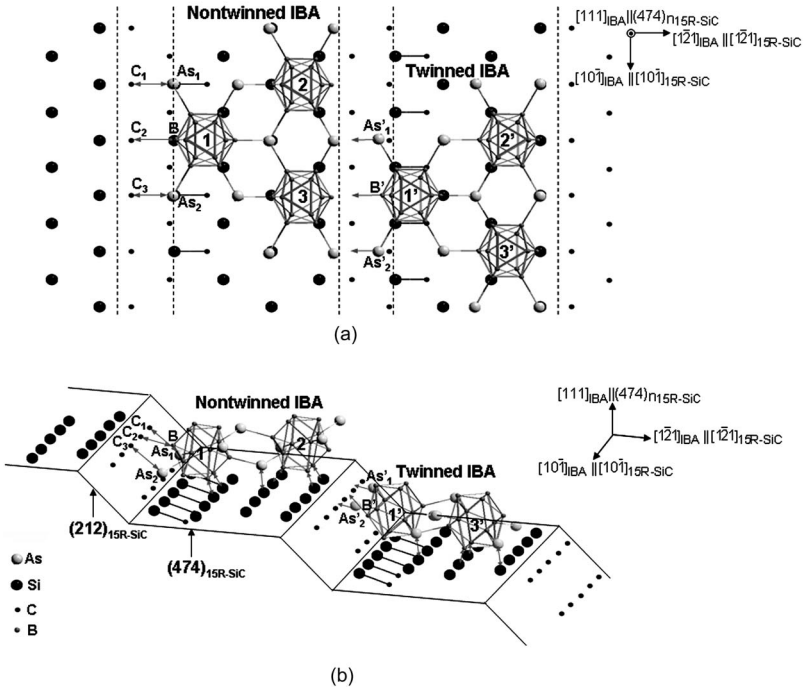

FIG. 4. (a) Plan view and (b) three-dimensional perspective view of nontwinned and twinned (353) IBA nucleated on *m*-plane 15*R*-SiC surface facets. For the nontwinned IBA, the triangular configuration of B atoms at the bottoms of icosahedra 1, 2, and 3 bond to the similarly oriented triangular configurations of Si atoms exposed on the $(474)_{15R\text{-}SiC}$ terrace [see (a) and (b)]. In addition, atoms As_1, B, and As_2 can be well bonded to atoms C_1, C_2, and C_3, respectively, on the neighboring $(212)_{15R\text{-}SiC}$ step riser. In contrast, while the triangular configuration of B atoms at the bottoms of icosahedra 1′, 2′, and 3′ can similarly bond to the $(474)_{15R\text{-}SiC}$ terrace, atoms As'_1, B′, As'_2 are not able to reasonably bond to the corresponding C atoms on the neighboring $(212)_{15R\text{-}SiC}$ step riser.

Growth then proceeds via step flow, whereby the IBA layer nucleated on one facet overgrows that nucleated on the facet below. This is possible since the spacing of the $(111)_{IBA}$ planes is within 15% of the height difference between adjacent $(474)_{15R\text{-}SiC}$ facets. Help in accommodating this 15% out-of-plane disregistry between is provided by the periodic presence of the deeper step riser comprising the coupled $(212)_{15R\text{-}SiC}$ and $(11\cdot8\cdot11)_{15R\text{-}SiC}$ facets. In addition, the in-plane lattice mismatch (~3.7%) can be well accommodated by the periodic appearance of interfacial dislocations [with one extra (555) half-plane on the SiC side, see examples on Fig. 2]. Thus, both in-plane and out-of-plane mismatch is accommodated. For monolayer IBA nucleated on adjacent $(474)_{15R\text{-}SiC}$ terraces, there is a small mutual sideways disregistry along the terrace of $1/4[10\bar{1}]_{IBA}$ (equivalent to $1/12[11\bar{2}0]_{IBA}$ in the hexagonal system). This is thought to be small enough that it can be accommodated elastically. For example, perfect registry will be attained if successive layers displace in opposite directions by $1/8[10\bar{1}]_{IBA}$. Partial nucleation on the narrower $(474)_{15R\text{-}SiC}$ facet just below the deeper step riser is expected to facilitate the overgrowth process between nuclei originating on the two broader $(474)_{15R\text{-}SiC}$ facets just above and below this narrower $(474)_{15R\text{-}SiC}$ facet. In this way, the IBA is able to quickly self-adjust its structure near the film/substrate interface while maintaining good bonding with the substrate, allowing it to subsequently grow with nearly perfect structure (see Fig. 2).

In conclusion, epitaxial growth of IBA on *m*-plane 15*R*-SiC substrates has been studied. SWBXT and cross-sectional HRTEM revealed untwinned (353) orientated IBA, with significantly improved macroscopic properties as probed optically. It was found that the choice of film orientation resulted from the tendency to nucleate in $(111)_{IBA}$ orientation on $(474)_{15R\text{-}SiC}$ close-packed facets.

Financial support from the National Science Foundation Materials World Network Program under Grant No. 0602875 and by the Engineering and Physical Science Research Council (EPSRC) under Grant No. EP/D075033/1 under the NSF-EPSRC Joint Materials Program is acknowledged. The SWBXT was carried out at Stony Brook Topography Facility (Beamline X19C) at the National Synchrotron Light Source (NSLS), Brookhaven National Laboratory (BNL), which is supported by the U.S. Department of Energy (D.O.E.) under Grant No. DE-AC02-76CH00016. Research carried out (in part) at the Center for Functional Nanomaterials, BNL, which is supported by the U.S. Department of Energy, Division of Materials Sciences and Division of Chemical Sciences, under Contract No. DE-AC02-98CH10886.

[1] D. Emin, Phys. Today **40**, 55 (1987).
[2] M. Carrard, D. Emin, and L. Zuppiroli, Phys. Rev. B **51**, 11270 (1995).
[3] D. Emin, J. Solid State Chem. **177**, 1619 (2004).
[4] D. Emin and T. L. Aselage, J. Appl. Phys. **97**, 013529 (2005).
[5] J. R. Michael, T. L. Aselage, D. Emin, and P. G. Kotula, J. Mater. Res. **20**, 3004 (2005).
[6] D. Emin, J. Solid State Chem. **179**, 2791 (2006).
[7] R. H. Wang, D. Zubia, T. O'Neil, D. Emin, T. Aselage, W. Zhang, and S. D. Hersee, J. Electron. Mater. **29**, 1304 (2000).
[8] W. M. Vetter, R. Nagarajan, J. H. Edgar, and M. Dudley, Mater. Lett. **58**, 1331 (2004).
[9] R. Nagarajan, Z. Xu, J. H. Edgar, F. Baig, J. Chaudhuri, Z. Rek, E. A. Payzant, H. M. Meyer, J. Pomeroy, and M. Kuball, J. Cryst. Growth **273**, 431 (2005).
[10] X. Zhou, J. H. Edgar, and S. Speakman, J. Cryst. Growth **293**, 162 (2006).
[11] H. Chen, G. Wang, M. Dudley, L. Zhang, L. Wu, Y. Zhu, Z. Xu, J. H. Edgar, and M. Kuball, J. Appl. Phys. (to be published).
[12] S. W. Chan, J. Phys. Chem. Solids **55**, 1137 (1994).
[13] C. P. Flynn and J. A. Eades, Thin Solid Films **389**, 116 (2001).
[14] H. Chen, G. Wang, M. Dudley, L. Zhang, L. Wu, Y. Zhu, Z. Xu, J. H. Edgar, and M. Kuball (unpublished).
[15] J. Takahashi, N. Ohtani, M. Katsuno, and S. Shinoyama, J. Cryst. Growth **181**, 229 (1997).